

CORROSION MONITORING ON STAINLESS STEEL UNDER CONDENSING NITRIC ACID CONDITIONS.

K.Hladky¹, D.G.John¹, S.E.Worthington² and D.Herbert².

¹ Corrosion and Protection Centre Industrial Services (CAPCIS)
University of Manchester Institute of Science and Technology (UMIST)

² British Nuclear Fuels Plc

Abstract.

Electrochemical monitoring techniques such as a.c. impedance, electrochemical noise and galvanic coupling have been applied to the monitoring of corrosion attack on 304L stainless steel under condensing HNO₃ conditions. A multi-system monitoring approach incorporating the above electrochemical techniques together with temperature and pressure monitoring has been used, employing specially designed multi-element probes, electronics and extensive computerised data logging and analysis. Measurements have been carried out in both a full scale evaporator rig and in a laboratory test rig over a range of temperatures and condensate compositions.

Introduction.

Corrosion under condensing conditions, particularly in condensing acids, is a complex phenomenon, dependent on numerous parameters, including the presence or otherwise of surface films, oxygen level, condensate pH, rate of condensate formation or removal etc. In many cases the precise conditions leading to the formation of the condensate are not readily calculable, as these depend on complex relationships of temperature, pressure, vapour composition and other variable parameters.

Previous experience in sulphuric acid dewpoint corrosion monitoring on mild steel^{1,2} has shown that data relating to corrosion tendency, including the onset of corrosion, corrosion type and relative corrosivity of the condensate can be obtained by continuous electrochemical monitoring via flush mounted, multi-element laminar probes³ and by the simultaneous monitoring of several electrochemical signals.^{4,5}

The Corrosion and Protection Centre Industrial Services (CAPCIS), University of Manchester Institute of Science and Technology (UMIST) together with British Nuclear Fuels Plc are applying this approach to the study of corrosion in a Lessing ring disentrainment bed in a full scale nitric acid evaporator rig as a part of a materials selection exercise. Concurrent tests are also in progress on a smaller laboratory test rig. In both cases specially designed multi-element probes are inserted into the packed evaporator column and are used, with analogue electronic monitoring equipment and computerised data logging and analysis facilities (CAPCIS 'MUSYC' monitor and 'ALFRED' software), to study the variations in the corrosion behaviour of the selected test material.

Insertion Probes and Test Rigs.

The general arrangement and size of the multi-element insertion probes, as shown in Fig.1, have remained the same throughout the test programme; different numbers and sizes of test elements, insulator types and spacings have been tried. The current design (40 mm diameter, 450 mm total length) incorporates twelve 10 mm wide elements with 5 mm wide PVDF insulators. Type K thermocouples are also incorporated into each probe. One of the pair of probes inserted into the full scale rig also contains a noble metal reference electrode for d.c. corrosion potential measurement.

Problems were experienced in selecting an appropriate material for the element spacers, as they need to be both chemically resistant to the condensate, over the expected range of temperatures, and to have favourable surface wetting properties in order to allow the condensate to bridge the insulators. Research is still continuing in this area and

materials such as polypropylene, PTFE, PVDF, glass filled PTFE and Macor (machineable ceramic) are being tested. The current design incorporates an open weave glass-fibre tape wrapped around the probe to assist condensate hold-up. It is accepted that this alters the conditions at the probe surface. This may affect the accumulation of corrosion products, give rise crevice geometries and so possibly distort the rates of the corrosion processes.

On the full size evaporator rig two probes were installed horizontally into the Lessing ring column through stainless steel cages (Fig.2). In addition to the various electrochemical parameters and temperatures the rig pressure was also monitored using a calibrated stainless steel pressure transducer.

The laboratory test rig was constructed from QVF glassware, comprising a 150 mm end-cap attached to a T-piece packed with 504L and glass rings. The multi-element probe was inserted into the sidearm of the T-piece which was then packed with the Lessing rings. An electric heater, a large reflux condenser and a vacuum pump completed the assembly (Fig.3).

Monitoring and Recording Systems.

The probes were connected by a multicore cable to the CAPCIS designed modular monitoring system. This was housed in a large air-conditioned enclosure adjacent to the full scale evaporator rig. The enclosure also housed the BBC computer and associated hardware and a battery backup unit (Fig.4). The laboratory monitor was a free-standing CAPCIS 'MUSYC' box device.

The electrochemical monitoring techniques used included a.c. impedance, electrochemical noise, galvanic coupling current and, in the case of the full scale evaporator, d.c. corrosion potential monitoring. The various techniques and the system as a whole have been described previously³⁻⁶ and are summarised below. The general arrangements of the monitoring systems are shown in Fig.5.

The electrochemical a.c. impedance module uses a two-frequency perturbation to measure the test cell impedance at 0.1 Hz and 10 kHz. Since the 10 kHz measurement determines the solution resistance (R_s) and the 0.1 Hz measurement gives the combined solution and charge transfer resistance ($R_s + R_{ct}$) the difference between the two measurements gives an estimate of the charge transfer resistance of the test cell, from which the corrosion rate may be determined using Stern-Geary type of analysis.⁷ The technique is a simplification of the full frequency scan as normally carried out with a frequency response analyser⁷, and as such suffers from several limitations. Since only two frequencies are employed, increased errors are introduced in situations where these are not adequately representative of the overall a.c. behaviour of the test cell over a wide frequency range. This is the case if the complex plane response of the cell differs significantly from a simple charge transfer semicircle or if the time constant of the cell differs from that for which the module design had been optimised.

The advantage of this approach is that it offers a simple means of estimation of the charge transfer impedance of the test cell. It also tracks the sharp changes in the solution resistance component of the cell impedance which are often found in condensing systems.

The electrochemical potential noise module measures the low level fluctuations of the potential between the two test electrodes at a frequency of approximately 50 mHz. The output of the module is proportional to the logarithm of the rms value of the signal over an amplitude range of 1 μ V to 10 mV. Experience has shown that the technique is sensitive to the initiation stage of pitting or crevice corrosion and as such provides valuable information relating to the onset and propagation of localised corrosion.⁴

The galvanic coupling module is essentially a sensitive zero resistance ammeter (ZRA) and is set up to measure the coupling current between two similar test electrodes. The output of the module is proportional to the logarithm of the absolute value of the coupling

current over a range of 0.1 μA to 1 mA. This technique is sensitive to the later stages of pitting or crevice attack as well as to general corrosion. The value of the ZRA current can be empirically related to the rate of attack.⁴

The d.c. corrosion potential module simply measures the potential difference between a gold wire reference electrode and a 304L probe element. It was found that the potential of gold remains relatively stable in the present system but research is continuing into the possibility of using other noble metal/oxide reference electrodes.

Temperatures were monitored with type K thermocouples connected to either thermocouple amplifiers (on the full scale rig) or directly to the Chessell 506 recorder. The operating pressure of the rigs was also monitored using suitable pressure transducers and signal conditioning electronics.

In all cases the data was logged onto Chessell 306 six-channel multi-point recorders. For the full scale evaporator system monitoring two sets of electronic modules and two recorders were used. The strip-chart recorders provide a permanent record of the data, serving as a useful backup of the computerised logging system. The data was digitised either by the recorder itself, in the case of the laboratory monitor, or by a Biodata Microlink 32 channel, 12 bit A/D device. The interface to the computer was via a RS-232 link in the former case and via a IEEE-488 interface on the full scale rig. The digitised data was pre-processed on the BBC microcomputer and stored on floppy disk in a format designed to optimise to available storage space; the 'ALFRED' software stores either 2 or 4 hour data files, sampling the input data every 15 seconds. The 'ALFRED' package also includes the calculation of routine statistical parameters and hard copy plotting of user selected portions of the recorded data and of long term data summaries.

Previous work has shown that the simultaneous measurement of several electrochemical parameters tends to increase both the amount and the reliability of the information produced by the monitoring process. The techniques overlap in their areas of applicability; electrochemical noise is sensitive to the initial stages of film breakdown and localised corrosion initiation, whereas ZRA current monitoring operates best during the later stages of the localised attack, a.c. impedance measurement provides information of the average rate of attack. This approach may be complemented by the measurement of other process parameters and by computer assisted analysis, often revealing previously hidden interrelations in the data and helping to pinpoint dangerous combinations of process parameters.

Experimental Results and Discussion.

Typical results for a test run on the laboratory rig are shown as detailed single data file plots in Fig.6 and Fig.7 and as a summary plot in Fig.8. These relate to a test run on the laboratory rig, using 12M HNO_3 , 304L stainless steel and covering a period of ca. 15 days.

During the test the temperature of the probe was varied by changes in the rate of heating and rig pressure, and by the addition or removal of lagging from the probe zone of the rig. These parameters affect the rate of deposition and the composition of the condensate in the probe area.

Corrosion and process data for the whole test period are summarised in Fig.8. This shows the mean of the plotted parameter, the superimposed vertical bars indicate +/- deviation of the data from this mean within each 4 hour data file. From the data as presented here it can be seen that a degree of correlation exists between the various electrochemical techniques, the rig pressure and the probe temperature.

The first quarter of the data relates to a time when the rig pressure and the probe temperature were adjusted to give highly corrosive conditions in the probe zone. These conditions were then held constant for the next quarter of the record in Fig.8. The test conditions were then again varied in order to see if low corrosion rates of the probe

material could be restored. This was followed by further short term cycling over the last quarter of the data.

It can be seen that the potential noise signal exhibits greatest fluctuation (largest vertical bars) in the first and third quarters of the data. This is also reflected on the ZRA trace and corresponds to conditions of greatest likelihood of localised attack.

Detailed examination of the recorded data is also possible with the 'ALFRED' software. Fig.6 shows data obtained during steady state operating conditions at 100°C. Moderately high electrochemical noise levels are present; these together with a low value of R_{ct} and a high value of the ZRA current indicate a fast uniform corrosion attack of ca. 1 mm/year. Subsequent reduction in temperature gave data shown in Fig.7, the electrochemical impedance (R_{ct}) reading is an order of magnitude higher, the electrochemical noise activity is low and the ZRA current is near the low limit of sensitivity of the instrument (1 μ A), corresponding to a corrosion rate of <0.005mm/yr. Secondary experiments calibrating the ZRA and R_{ct} against linear polarisation had given reasonable correlation with the ZRA up to high corrosion currents (>250 μ A), but a poor correlation with R_{ct} . This probably reflected the need to use a lower frequency for the second monitoring value for R_{ct} .

Full a.c. impedance scans were carried out periodically during the test run, an example being given in Fig.9. The time at which it was taken is indicated by the arrow in Fig.8. The scans shown were taken on probe rings at different positions in the packed bed. It can be seen that although relatively high corrosion rates are occurring at three positions (up to 0.5mm/yr), the fourth is showing passive behaviour. This was situated in the entrance port at the side of the vessel and was consequently cooler and subject to different condensate conditions.

The measured corrosion rates at 100°C appear to be surprisingly high if compared to immersion test rates in bulk liquor.⁸ However, as was pointed out earlier the glass mesh enclosing the probe, and the interfaces between the probe elements and insulators give rise to crevice geometries. Enhanced crevice corrosion rates have been reported previously in nitric acid.⁹ Other possible supplementary causes are increasing acidities in the condensate due to fractionation effects, and build up of aggressive corrosion products in the condensate films. It is intended to assess the latter effects in subsequent experiments by sampling the condensates.

Fig.10 summarises a series of runs on the full scale evaporator rig using 6M HNO_3 . This lower acidity gave lower corrosion rates for most of the test duration (<0.005 mm/yr at 50°C and <0.05 mm/yr at 100°C), however, towards the end of the run one of the ZRA elements gave a high reading, indicating the possible development of crevice corrosion as at this acid molarity the incubation time for crevice corrosion development would be expected to be longer than for 12M HNO_3 . Although the correlations of the readings from this rig were less clear than those from the small scale rig there is still a good evidence of a relationship between the electrochemical data and the temperature profile.

Conclusions.

The present work has shown that it is feasible to monitor corrosion processes in a condensing HNO_3 system. By the use of suitable multi-element insertion probes and by the application of a multi-system monitoring approach backed up with computer assisted data processing facility it is possible to begin to identify those combinations of process parameters which result in unacceptable corrosion behaviour.

This extends our previous experience of applying continuous multi-system corrosion monitoring, which had been gained chiefly in H_2SO_4 dewpoint situations, and increases our confidence in the validity of this type of approach to corrosion monitoring.

Although there are still some specific areas which require further investigation, both BNFL and CAPCIS feel that the present monitoring exercise has helped us to understand some

of the problems involved in applying novel electrochemical monitoring techniques and approaches to an industrial situation.

Acknowledgements.

The authors would like to acknowledge the contributions from other members of both organisations, in particular Dave Eden and Pete Aylott of CAPCIS and John Harrison and Debbie Keighley of BNFL Windscale.

References.

1. W.M.Cox, J.L.Dawson, D.Gearey, Paper presented at UK/Corrosion 82, London, November 1982
2. W.M.Cox, D.M.Farrell, J.L.Dawson, Dewpoint Corrosion, D.R.Holmes ed., Ellis Horwood, p191
3. W.M.Cox, J.L.Dawson, P.C.Searson, UK Patent Application No. 8510015
4. K.Hladky, J.P.Lomas, D.G.John, D.A.Eden, J.L.Dawson, Corrosion Monitoring and Inspection in the Oil, Petrochemical and Process Industries 1984, Oyez Scientific and Technical Services Ltd., p211
5. J.L.Dawson, D.A.Eden, K.Hladky, On-line Monitoring of Continuous Process Plant, D.W.Butcher ed., Ellis Horwood Ltd., p119
6. D.G.John, D.A.Eden, K.Hladky, J.L.Dawson, Paper presented at NACE Corrosion 84, Science Research Symposium, New Orleans, USA, April 1984
7. K.Hladky, L.M.Callow and J.L.Dawson, Br.Corr.J., 15, p20 (1980)
8. A.J.Sedricks, Corrosion of Stainless Steels, J.Wiley & Sons Inc., p221
9. J.M.Harrison, R.J.Andon, R.C.Pemberton, J.G.N.Thomas, S.E.Worthington, R.D.Shaw, Paper presented at UK Corrosion 1984, London

Figures.

1. General Multi-element Electrochemical Probe Arrangement.
2. Probe Shield Arrangement on the Full Scale Test Rig.
3. Laboratory Test Rig.
4. Arrangement of Data Logging System for Full Scale Evaporator Rig.
5. Block Diagram of the Monitoring System.
6. Single Data File Computer Generated Printout (Laboratory Rig).
7. As Fig.6, later data.
8. Long Term Data Summary from a Laboratory Rig Run.
9. A.c. Impedance Scans from a Laboratory Rig Run.
10. Long Term Data Summary from a Full Scale Rig Run.

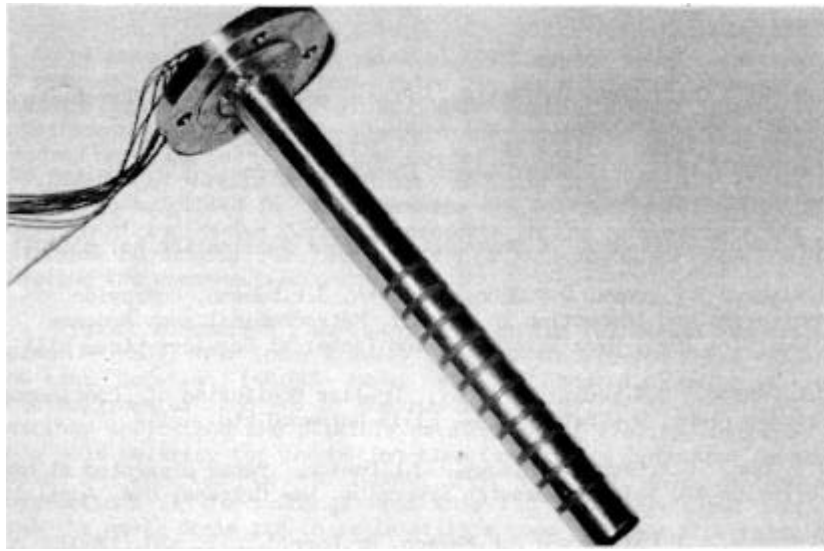


Figure 1. General Multi-element Electrochemical Probe Arrangement.

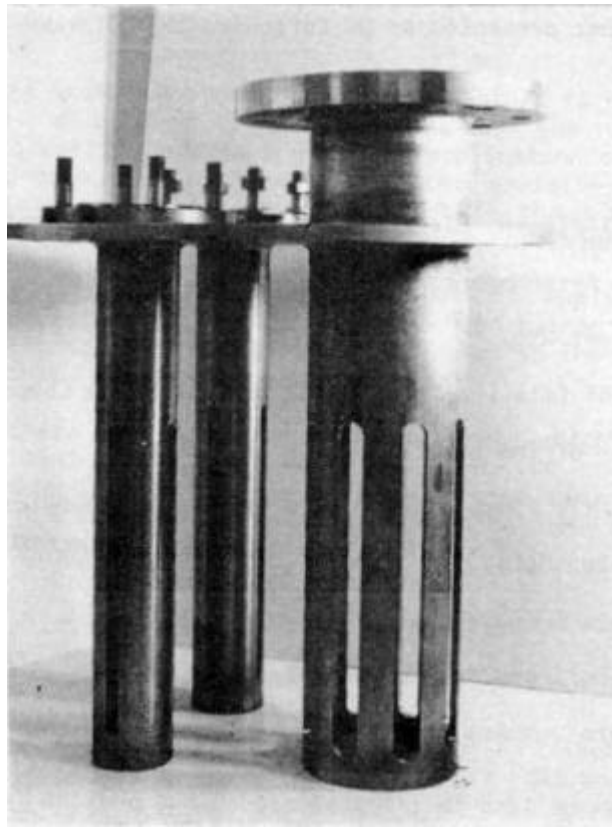


Figure 2. Probe Shield Arrangement on the Full Scale Test Rig.

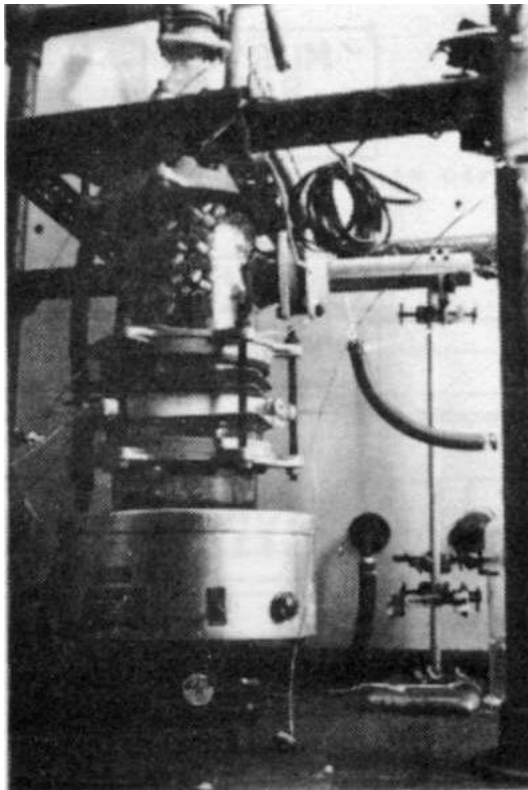


Figure 3. Laboratory Test Rig.

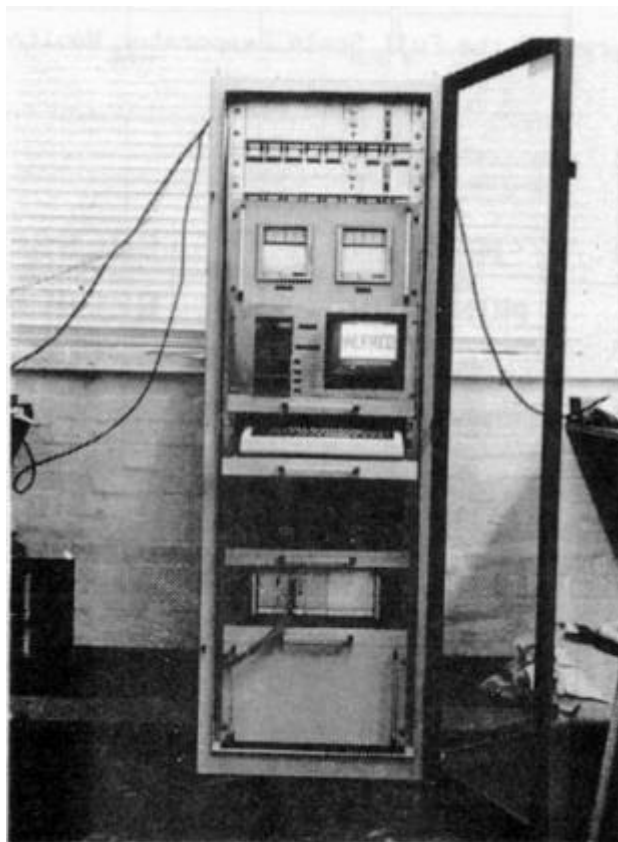


Figure 4. Arrangement of Data Logging System for Full Scale Evaporator Rig.

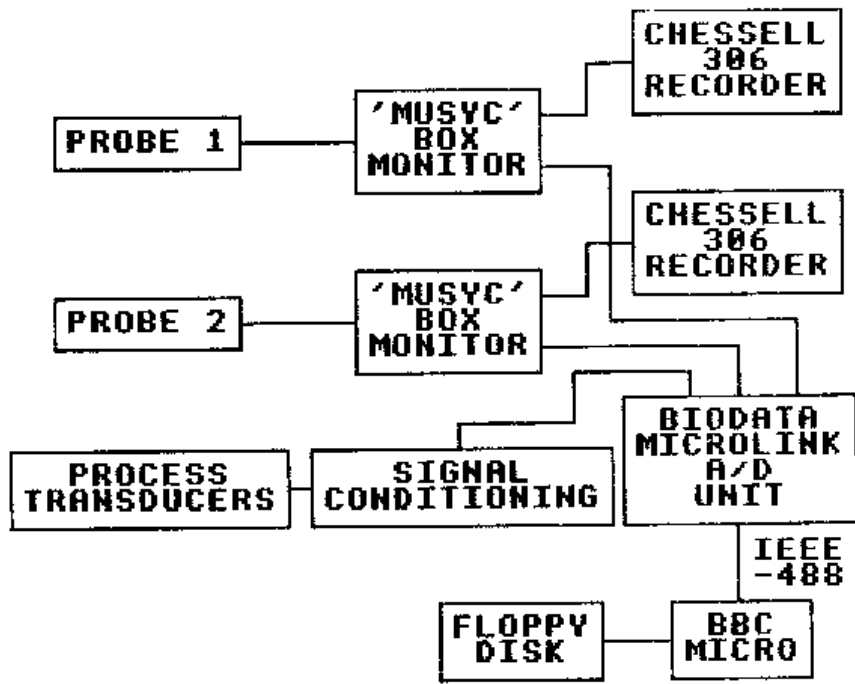


Figure 5a. Block Diagram of the Full Scale Evaporator Monitoring System.

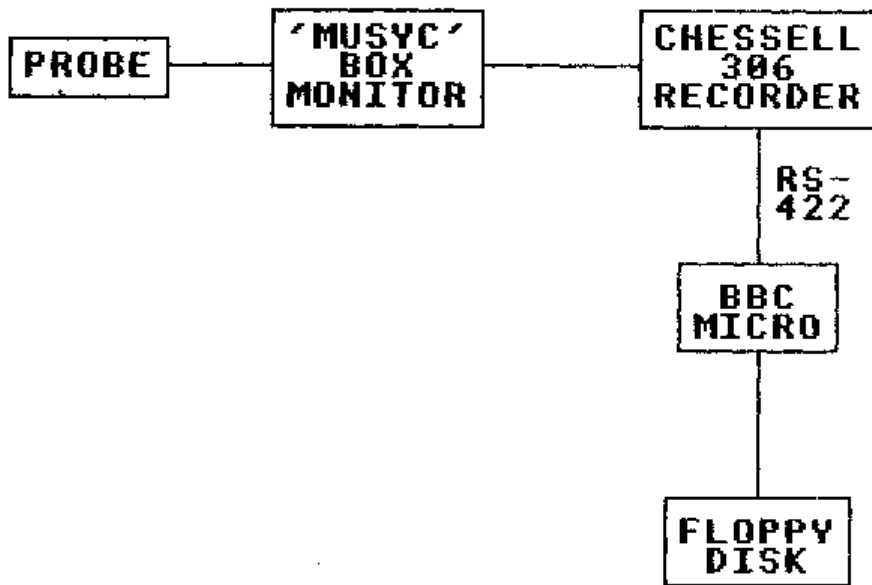


Figure 5b. Block Diagram of the Laboratory Rig Monitoring System.

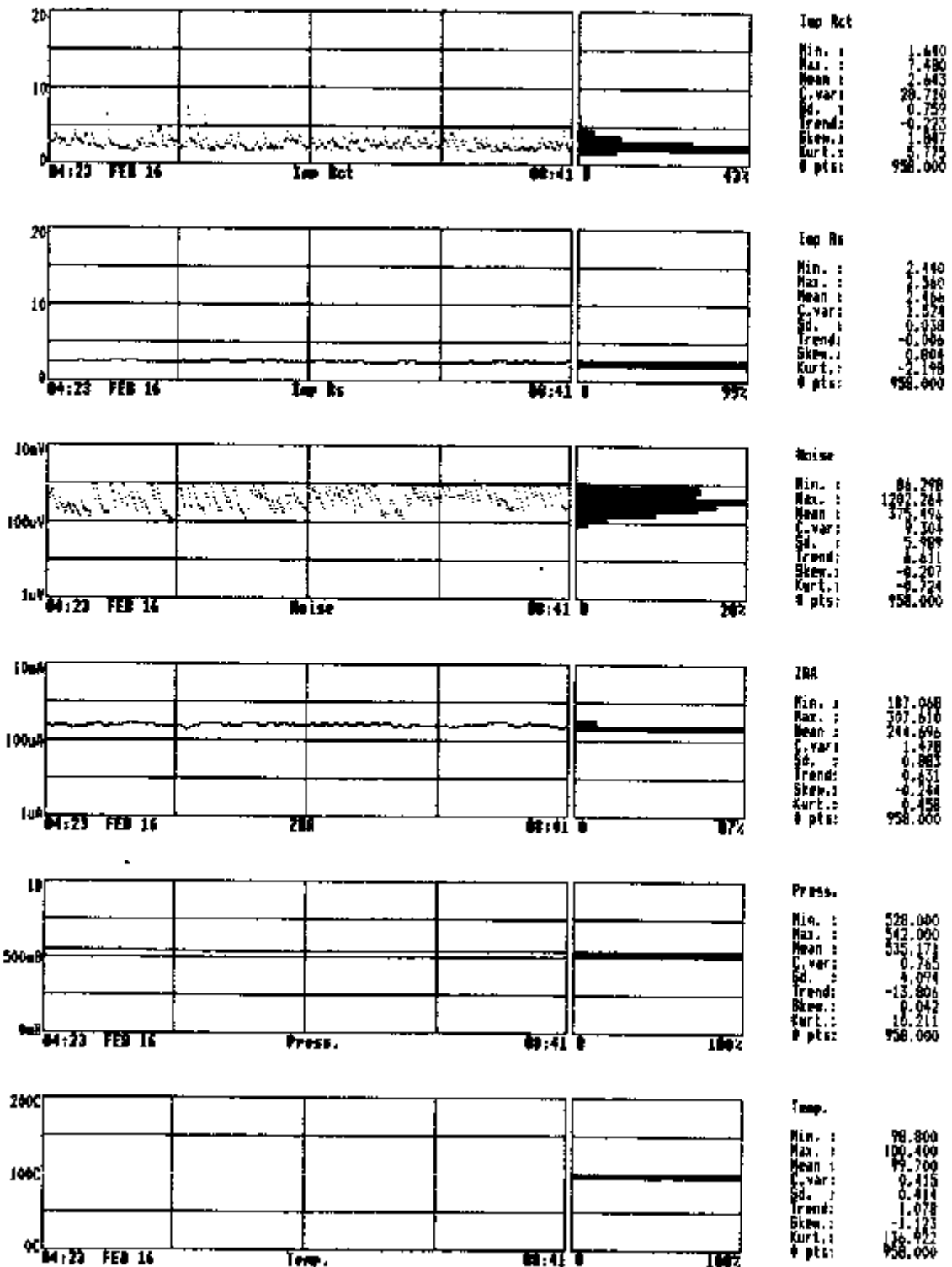


Figure 6. Single Data File Computer Generated Printout (Laboratory Rig).

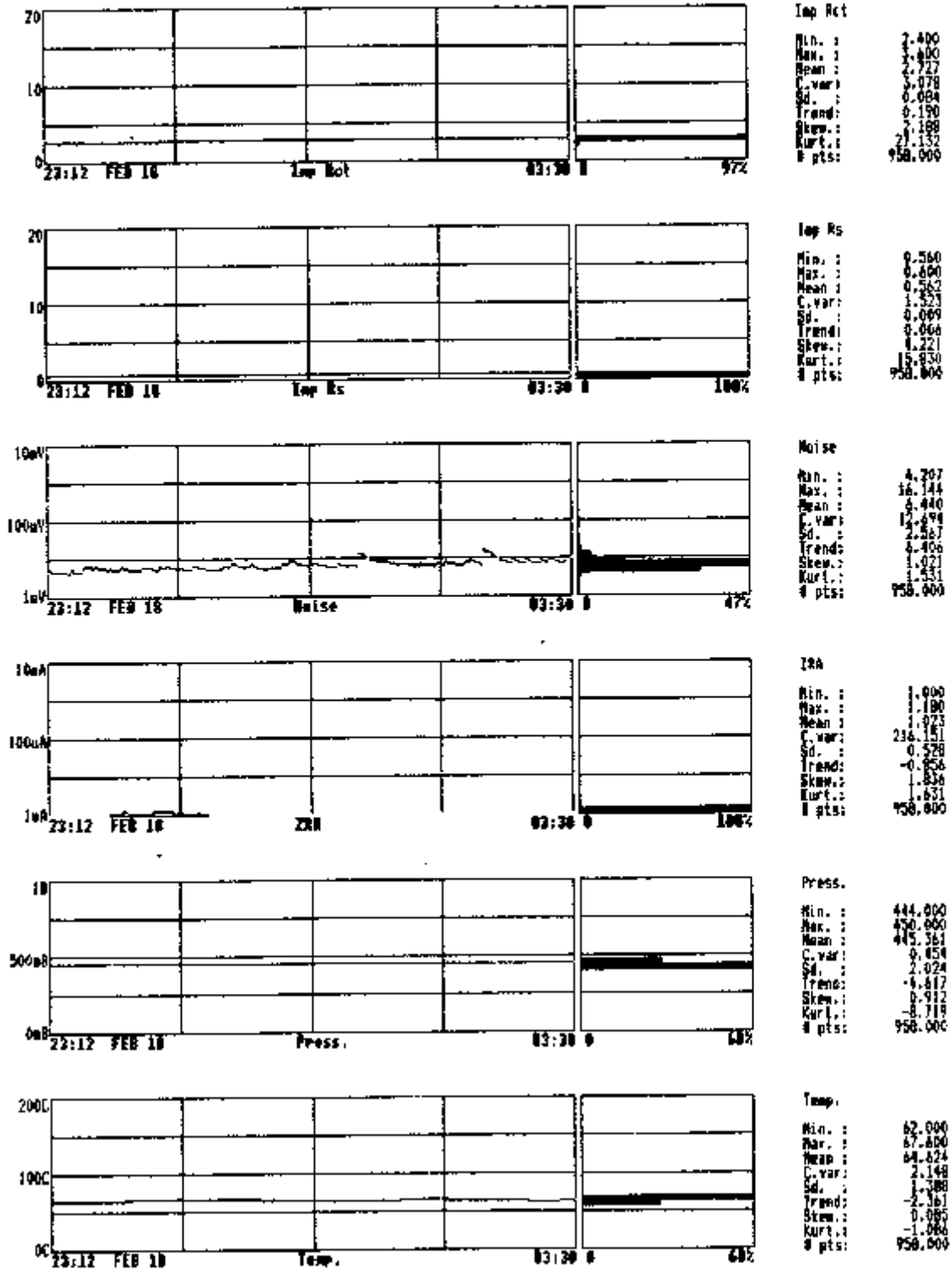


Figure 7. As Fig.6, later data.

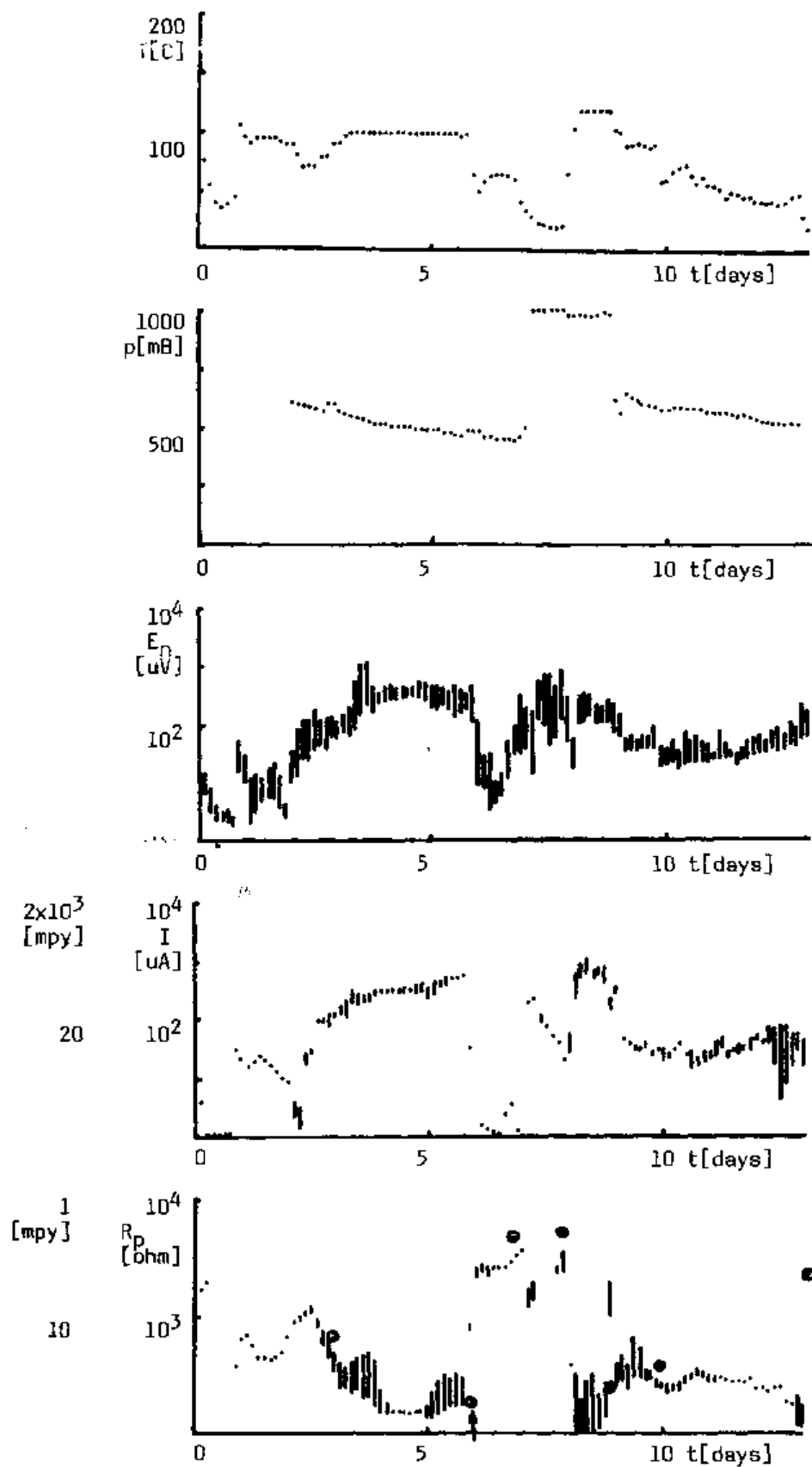


Figure 8. Long Term Data Summary from a Laboratory Rig Run.

BNFL3 LAB RIG PROBE IMPEDANCES 18/2/85 T=100C P=500mB

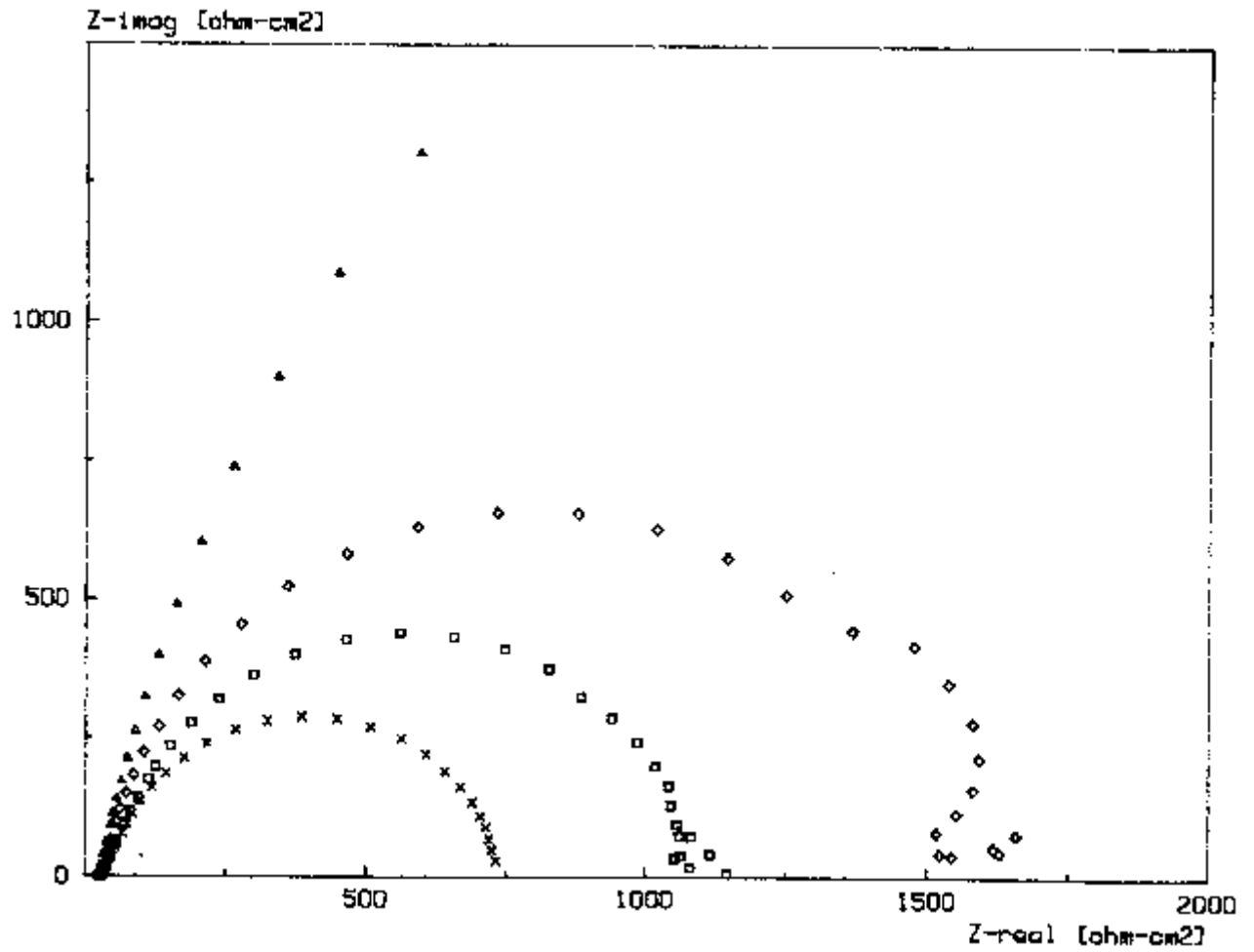
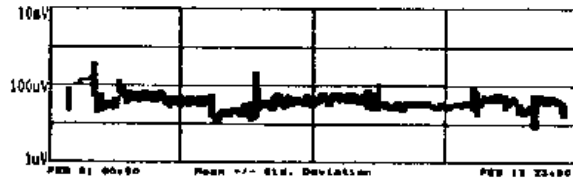
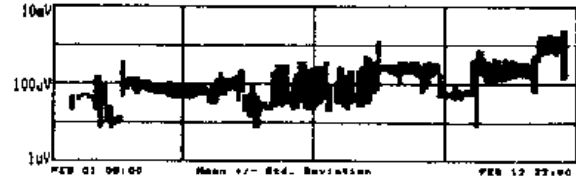


Figure 9. A.c. Impedance Scans from a Laboratory Rig Run.

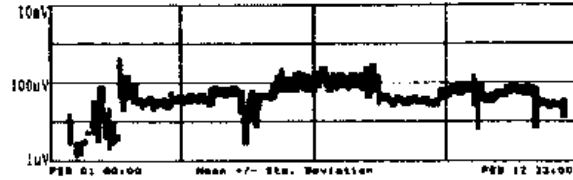
CAPCIS - Probe 1: noise 1



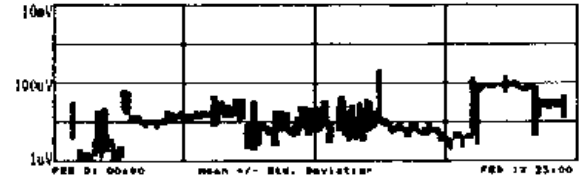
CAPCIS - Probe 2: noise 1



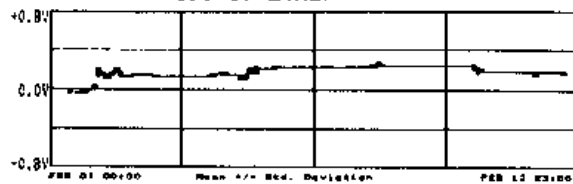
CAPCIS - Probe 1: noise 2



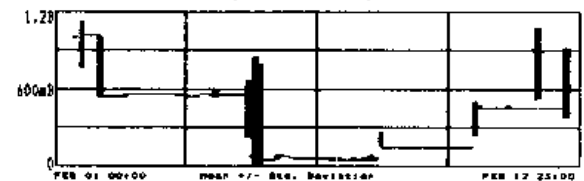
CAPCIS - Probe 2: noise 2



CAPCIS - Probe 1: E(Au)



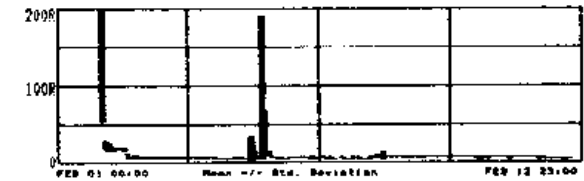
CAPCIS - Probe 2: Pressure



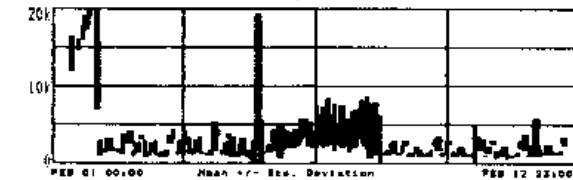
CAPCIS - Probe 1: Iap Rs



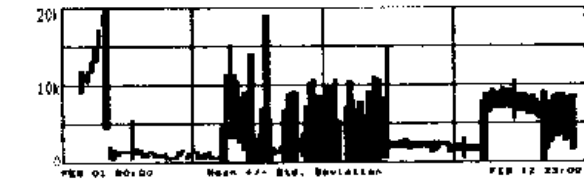
CAPCIS - Probe 2: Iap Rs



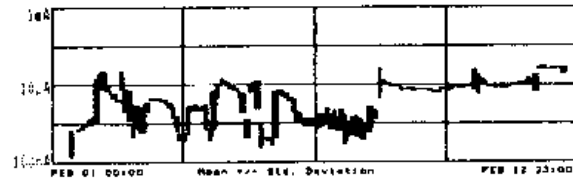
CAPCIS - Probe 1: Iap Rct



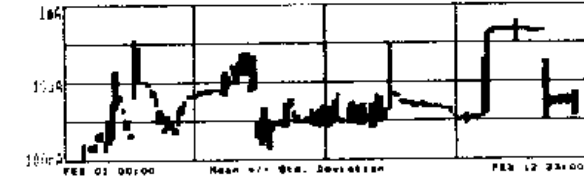
CAPCIS - Probe 2: Iap Rct



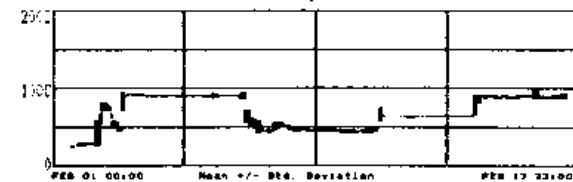
CAPCIS - Probe 1: ZRA



CAPCIS - Probe 2: ZRA



CAPCIS - Probe 1: Temp.



CAPCIS - Probe 2: Temp.

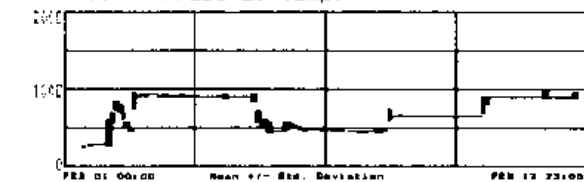


Figure 10. Long Term Data Summary from a Full Scale Rig Run.